Inorganic Chemistry

Article

pubs.acs.org/IC

New Nonlinear Optical Crystal: $NaBa_4Al_2B_8O_{18}Cl_3$

Jianxiu Zhang,[†] Shufeng Zhang,[†] Yicheng Wu,*[,†] and Jiyang Wang[‡]

[†]Key Laboratory of Functional Crystals and Laser Technology, Technical Institute of Physics and Chemistry, Chinese Academy of Sciences, Beijing 100190, China

[‡]State Key laboratory of Crystal Material, Shandong University, Jinan, 250100, China

Supporting Information

ABSTRACT: Single crystals of $NaBa_4Al_2B_8O_{18}Cl_3$ have been grown with sizes up to $34 \times 34 \times 16$ mm^3 from the NaF−LiCl flux by the top-seeded solution growth method. The compound crystallizes in the tetragonal system, space group $P4_2nm$, with a = 12.0480 (16) Å, c = 6.8165 (11) Å, $\alpha = \beta = \gamma = 90°$, and two formula units per cell. The $NaBa_4Al_2B_8O_{18}Cl_3$ compound is built up of infinite anionic groups of $[AlB_4O_{12}]^{9-}$ formed by two BO_4 tetrahedra, one AlO_4 tetrahedra, and two BO_3 triangles. Optical properties including ultraviolet transmission, IR spectrum, and second-harmonic generation of $NaBa_4Al_2B_8O_{18}Cl_3$ crystals were reported. Refractive indices were measured by the minimum deviation technique and fitted to the Sellmeier equations. Thermal properties such as the DSC and thermal expansion were reported. The mechanical properties including the hardness, density, and chemical stability were also reported.

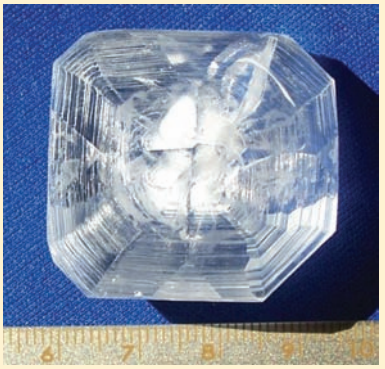

INTRODUCTION

Borate crystals are often employed for nonlinear optical (NLO) application, such as the third harmonic and fourth harmonic of a 1064 nm Nd:YAG laser, because of their high transparency in the UV region and high resistance against laser-induced damage.[1] In 1975, the first discovered borate NLO crystal $KB_5O_8{\cdot}4H_2O$-(KB_5) was successfully used for UV generation.[2] Afterward, borate crystals were intensely investigated. To date, series of borate NLO crystals, such as β-$Ba_2B_2O_4$(BBO),[3] LiB_3O_5(LBO),[4] CsB_3O_5(CBO),[5] and $YCa_4O(BO_3)_3$(YCOB),[6] have been discovered. Recently, we discovered a new borate crystal with composition $NaBa_4Al_2B_8O_{18}Cl_3$(NBAC). The NBAC crystals are found to be chemically stable and not hygroscopic. In this paper, we report the synthesis, crystal growth, and structure as well as the optical, thermal, and mechanical properties of NBAC.

EXPERIMENTAL SECTION

Synthesis and Crystal Growth. NBAC melts incongruently, and we have previously grown NBAC crystals in single NaF or LiCl flux separately.[7] However, few crystals with good quality were obtained. In order to obtain high-quality NBAC single crystals and study their optical and physical properties, we made efforts to find new flux to grow NBAC. In this paper, NaF−LiCl flux with a ratio of 2:1 was found to be an excellent flux to grow NBAC. In the experiment, polycrystalline samples of NBAC were prepared using solid-state reaction techniques with a stoichiometric mixture of NaCl, Na_2CO_3, $BaCO_3$, $BaCl_2{\cdot}2H_2O$, Al_2O_3, and H_3BO_3 (all analytical grade). The purity of the sample was checked by X-ray powder diffraction. A single-phase powder of NBAC was obtained when repeated heat treatment caused no further changes in the X-ray powder diffraction. The chemical equation can be expressed as follows

$$NaCl + 3BaCO_3 + BaCl_2{\cdot}2H_2O + Al_2O_3 + 8H_3BO_3 = NaBa_4Al_2B_8O_{18}Cl_3 + 14H_2O\uparrow + 3CO_2\uparrow \quad (1)$$

$$Na_2CO_3 + 5BaCO_3 + 3BaCl_2{\cdot}2H_2O + 2Al_2O_3 + 16H_3BO_3 = 2NaBa_4Al_2B_8O_{18}Cl_3 + 30H_2O\uparrow + 6CO_2\uparrow \quad (2)$$

It was mixed with NBAC, NaF, and LiCl to produce a mass ratio of NBAC:NaF:LiCl as 100:16:8. The mixture was ground carefully to ensure homogeneous mixing and then sintered for 24 h at 550 °C. Product was melted in a platinum crucible at 800 °C in batches. The furnace was heated rapidly to 880 °C and maintained for 24 h, and then it was cooled rapidly to 770 °C. A seed crystal of NBAC attached to a platinum rod was inserted slowly into the crucible and kept in contact with the surface of the solution, while a temperature of 775 °C was maintained for 0.5 h to dissolve the outer surface of the seed. The growing crystal was rotated at a rate of 15 rpm. The solution was then cooled rapidly to a saturation temperature of 770 °C determined by repeated seeding, and then the temperature was slowly reduced to 700 °C at a rate of 0.5−3 °C/day until the end of growth. The crystal thus obtained was drawn out of the solution surface, cooled to room temperature at a rate of 30 °C/h, and then slowly taken out from the furnace.

Element Content Determination. The Na, Ba, Al, B, as well as F^- and Cl^- contents in the crystal were determined using an ICP-OES plasma spectrometer and DIONEX ICS-3000 ion chromatograph, respectively.

Single-Crystal X-ray Diffraction. Single-crystal X-ray-diffraction data for the as-grown NBAC were collected with a Bruker P4 diffractometer equipped with Mo Kα X-radiation and a 1K CCD detector. Integrated intensities of 1650 reflections with $-16 < h < 16$, $-11 < k < 11$, and $-9 < l < 9$ were collected up to $2\theta = 60°$ using 60 s per frame. Refined lattice parameters of NBAC were obtained from

Received: February 11, 2012
Published: June 4, 2012

   dx.doi.org/10.1021/ic300306v | Inorg. Chem. 2012, 51, 6682−6686

1469 strong reflections ($I > 2\sigma$). Experimental parameters for data collection and refinement are given in Table 1. An empirical absorption correction (SADABS, Sheldrick 1998) was applied. The structure was solved with SHELXS-9714 by direct method and refined with SHELXL-9715 by full-matrix least-squares techniques with anisotropic thermal parameters for all atoms. The refined atomic positions and isotropic thermal parameters are given in Table S1 (see Supporting Information). The main interatomic distances are listed in Table S2 (see Supporting Information).

Table 1. Crystal Data and Structure Refinement for NBAC

formula	$NaBa_4Al_2B_8O_{18}Cl_3$
fw (g/mol)	1107.14
temp. (K)	293(2)
wavelength (Å)	0.71073
cryst sym	tetragonal
space group	$P4_2nm$
a	12.0480(16) Å
b	12.0480(2) Å
c	6.8165(11) Å
vol.	989.4(3) Å^3
Z	2
cald density (g/cm^3)	3.716
F(000)	992
abs coeff (mm^{-1})	8.458/mm
cryst size	0.2 mm × 0.2 mm × 0.3 mm
θ range for data collection	2.39−29.98°
index ranges	$-16 < h < 16$, $-11 < k < 11$, $-9 < l < 9$
reflns collected	1650
independent reflns	1534
independent reflns [$I > 2\sigma(I)$]	1469
R_{int}	0.0487
refinement method	full-matrix least-squares on F^2
no. of variable params	96
goodness-of-fit on F^2	1.057
final R indices [$I > 2\sigma(I)$]	R_1 = 0.0589, wR_2 = 0.1568
R indices (all data)	R_1 = 0.0603, wR_2 = 0.1588
largest diff. peak and hole (e·Å^{-3})	4.916 and −2.722

Second-Harmonic Generation Measurement. An optical second-harmonic generation (SHG) test was performed on the powder sample of NBAC by means of the Kurtz−Perry method. The fundamental wavelength is 1064 nm generated by a Q-switched Nd:YAG laser. The SHG wavelength is 532 nm. Microcrystalline KDP (KH_2PO_4) served as a reference.

Spectroscopy Measurement. The transmittance spectrum of NBAC was recorded at room temperature using a Perkin-Elmer Lambda 900 UV/vis/NIR spectrophotometer, which can operate over the range 175−3000 nm. The middle infrared (IR) spectrum was measured with the use of a Bio-Rad FTS165 spectrometer in the range of 400−4000 cm^{-1} on a 1 mm thick crystal at room temperature.

Refractive Indices Measurement. Refractive indices were measured by the minimum deviation angle method. Fifteen different wavelengths over the range of 404.7−1068 nm were used in the experiment. The sample was cut as a right-angle prism with an apex angle of about 30° and kept at 20 °C during measurement.

Thermal Properties Measurement. The thermal property was investigated by differential scanning calorimetric (DSC) analysis using the Labsys TG-DTA16 (SETARAM) thermal analyzer (the DSC was calibrated with Al_2O_3). About 10 mg of NBAC was used for the DSC measurement. The NBAC sample was placed in an Al_2O_3 crucible, and another empty Al_2O_3 crucible was used as the reference crucible as they were heated together at a constant rate of 20 °C/min from 25 to 1050 °C. The thermal expansion was measured in the temperature range from 20 to 300 °C using a thermal dilatometer RJY-2P(TMA). The crystal used for the thermal-expansion measurements was processed into a rectangular piece with dimensions of 6.9 × 6.8 × 8.0 mm^3 ($a \times b \times c$).

Microhardness Measurements. An MH-6 microhardness tester made by Hengyi Corp. in Shanghai was used to measure the Vickers microhardness of NBAC crystal at room temperature. For each load, the time of indentation was kept constant at 10 s and several indentations were made. The average value of the diagonal indentation length was used to calculate the Vickers microhardness. The samples consisted of two polished NBAC crystal wafers of 10 mm diameter having faces parallel to the (100) and (001) crystallographic planes.

Density Measurement. The density of the NBAC crystal was measured at 22 °C using the buoyancy method.

RESULTS AND DISCUSSION

Figure 1 shows the as-grown NBAC crystal with sizes up to 34 × 34 × 16 mm^3. It shows that the obtained crystal is colorless and partially transparent, and the crystal exhibits fairly distinguishable facets. We dipped a NBAC crystal weighting 1.000 g into water for 2 weeks, and the weight has almost no change, indicating that NBAC is chemically stable and not hygroscopic.

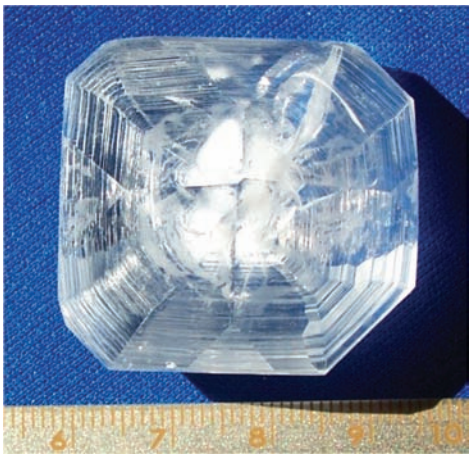

Figure 1. Photograph of NBAC crystal with sizes up to 34 × 34 × 16 mm^3 grown from NaF−LiCl flux.

Hardness is the resistance of a material to localized plastic deformation caused by indentation, scratching, cutting, or bending. Vickers microhardness is indentation hardness, which is determined as[8]

$$HV = 1.8544P/D^2 \quad (3)$$

where HV, P, and D are the Vickers microhardness value (kg/mm^2), applied load (g), and diagonal length of indentation (μm), respectively. The Mohs' hardness can be evaluated by the experienced formula: Mohs = $0.673(HV)^{1/3}$.[9] The Vickers hardness of NBAC was measured for loads of 100 g on different spots on the (100) and (001) crystallographic planes. The loading time is 10 s. The measured Vickers and calculated Mohs' microhardness are listed in Table 2. It can be seen that the microhardness of the (001) plane is slightly higher than that of the (100) plan. Generally speaking, the microhardness of single-crystal NBAC is moderate and easily processed.

The density of NBAC crystal can be calculated with the following equation

$$\rho = \frac{m}{V} = \frac{\rho_0}{[1 + (\Delta a/a_0)]\left[1 + \frac{\Delta b}{b_0}\right][1 + (\Delta c/c_0)]} \quad (4)$$

dx.doi.org/10.1021/ic300306v | Inorg. Chem. 2012, 51, 6682−6686

Table 2. Microhardness of NBAC Crystal

crystallographic plane	loading spots	*D*1 (um)	*D*2 (um)	*HV* (kg/mm^2)	average (kg/mm^2)	Mohs
(100)	1	17.4	20.0	530.3	571.4	5.58
	2	17.7	17.1	612.5		
(001)	1	17.2	17.4	619.6	610.8	5.71
	2	17.2	17.9	602.1		

where ρ_0 is the density of the crystal at T_0 and the values of $\Delta\alpha/\alpha_0$, $\Delta b/b_0$, and $\Delta c/c_0$ can be obtained from the later thermal expansion measurement. The experimental value for the density of the crystal at 22 °C is 3.66 g/cm^3, which is slightly smaller than the calculated value 3.71 g/cm^3.

NBAC crystallizes in the tetragonal system and belongs to the $P4_2nm$ space group with two formula units per cell. Its lattice parameters were measured to be a = 12.0480 (16) Å, c = 6.8165 (11) Å, $\alpha = \beta = \gamma = 90°$. Figure 2a, 2b, and 2c shows the crystal structure of NBAC projected along the [100] direction, [010] direction, and [001] direction, respectively. The structure of NBAC is a three-dimensional network of the infinite $[AlB_4O_{12}]^{9-}$ groups as shown in Figure 2d. From Figure 2d, we can see that the $[AlB_4O_{12}]^{9-}$ group is formed by one B(1)O$_4$ tetrahedra, one B(2)O$_4$ tetrahedra, two B(3)O$_3$ triangles, and one Al(1)O$_4$ tetrahedra with shared O atoms. The structural cavities in the $[AlB_4O_{12}]^{9-}$ backbone are filled with Ba, Cl, and Na, respectively. Ba cations are housed in the tunnels along the [100] and [010] directions as shown in Figure 2a and 2b, and whereas Cl and Na are located in the tunnels along the [001] directions as shown in Figure 2c. For B(1)O$_4$ tetrahedra, the B(1)−O bond lengths and O−B(1)−O bond angles are in the range 1.410(2)−1.490(2) Å and 107.8(9)−111.0(9)°, which are in good agreement with those reported previously for other borates such as $Na_3[B_6O_9(VO_4)]$[10] and $Ca_3Er_3Ge_2BO_{13}$.[11] The mean bond length and bond angle of B(1)O$_4$ units are 1.462(5) Å and 109.5(1)°, respectively. For B(2)O$_4$ tetrahedra, the B(2)−O bond lengths and O−B(2)−O bond angles are in the range 1.415(2)−1.531(1) Å and 101.6(1)−115.2(1)°. The mean bond length and bond angle are 1.484(5) Å and 109.3(8)°, respectively. For B(3)O$_3$ triangles, the B(3)−O bond lengths and O−B(3)−O bond angles are in the range 1.325(1)−1.396(1) Å and 118.7(8)−122.3(9)°. The mean bond length and bond angle are 1.368(5) Å and 120.0(5)°, respectively. For Al(1)O$_4$ tetrahedra, the Al(1)−O bond lengths and O−Al(1)−O bond angles are in the range 1.735(9)−1.772(1) Å and 107.7(4)−112.7(5)°, which are in good agreement with those reported previously for other aluminum borates such as $BaAlBO_3F_2$[12] etc. The mean bond length and bond angle of Al(1)O$_4$ units are 1.750(5) Å and 109.5(3)°, respectively.

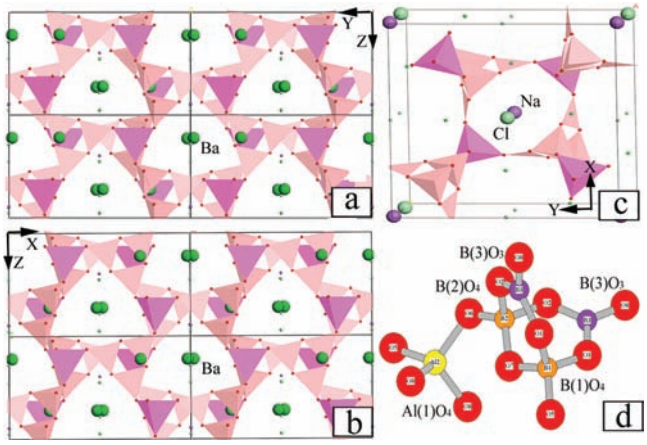

Figure 2. Crystal structure of NBAC. Framework projected along the (a) [100] direction, (b) [010] direction, and (c) [001] direction. (d) $[AlB_4O_{12}]^{9-}$ group.

NBAC has potential application for harmonic generation since it crystallizes in a noncentrosymmetric space group. On the basis of anionic group theory, the nonlinearity of a borate crystal originates in the boron−oxygen groups. NBAC was expected to possess a SHG effect because it contains BO$_3$ and BO$_4$ groups. In fact, green light was observed in our SHG experiment, and its intensity was slightly weaker than that of KDP when NBAC was ground into powder and loaded into a quartz cell, indicating that the powder nonlinear optical effect of NBAC is slightly lower than that of KDP.

Optical properties were measured on the crystal. Samples were cut in a thickness of 2 mm along the c axis from the as-grown NBAC crystal and then polished on diamond-impregnated laps. Figure 3 shows the transmission spectrum,

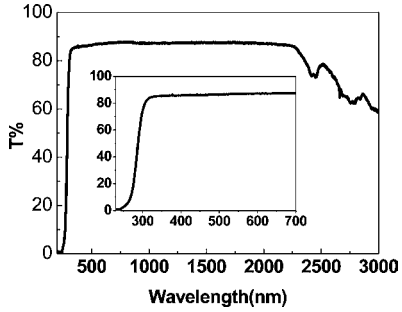

Figure 3. Transmission spectrum of NBAC crystals.

and we can see that a wide transmission range is observed in the UV to IR region. From the inset in Figure 3, it can be seen that the UV absorption edge is lower than 230 nm, indicating that it might be useful in UV frequency conversion applications.

Figure 4 shows the IR spectrum of NBAC. The IR spectrum of NBAC was assigned on the basis of results obtained from the vibration spectra measurements of other borate groups. The strong absorption bands at 1050.3 and 1385.2 cm^{-1} are related to the asymmetric stretching vibrations of BO$_4$ and BO$_3$ groups, respectively. In the 420−484 cm^{-1} region there are six apparent absorption bands, which are expected to be the out-of-plane bending vibrations of the BO$_4$ and AlO$_4$ groups. The absorption band at 715.3 cm^{-1} is related to the out-of-plane bending vibrations of BO$_3$ groups. The in-plane bending vibrations of BO$_4$ and BO$_3$ groups are observed in the IR spectrum, which correspond to the regions 506−592 and 633−678 cm^{-1}, respectively. The absorption bands at 880.6 and 993.3 cm^{-1} are related to the symmetric stretching vibrations of BO$_4$ and BO$_3$ groups. The observed bands and assignments are

dx.doi.org/10.1021/ic300306v | Inorg. Chem. 2012, 51, 6682−6686

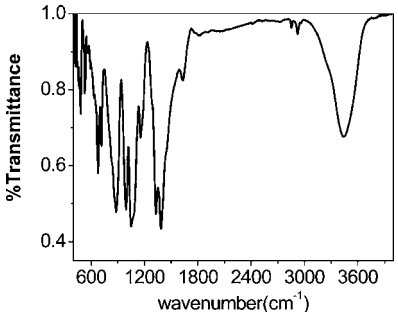

Figure 4. Infrared spectrum of NBAC.

listed in Table 3. Obviously, the NBAC crystal contains planar BO_3 and tetrahedral BO_4 and AlO_4 groups as its basic structural units.

Table 3. Band Assignments in the IR Spectrum of NBAC

wavenumber (cm^{-1})	assignments	wavenumber (cm^{-1})	assignments
633.6, 677.7	$BO_3(\nu_4)$	506.9, 528.3, 559.6, 591.7	$BO_4(\nu_4)$
715.3	$BO_3(\nu_2)$	420.6, 430.8, 443.2, 451.8	$BO_4(\nu_2)$
		464.0, 483.9	$AlO_4(\nu_2)$
993.3	$BO_3(\nu_1)$	880.6	$BO_4(\nu_1)$
1326.2, 1385.2	$BO_3(\nu_3)$	1050.3	$BO_4(\nu_3)$

As NBAC is the uniaxial crystal, it is possible to measure both n_o and n_e using one crystallographically oriented single-crystal prism. The optic Z axis (coincident with the crystallographic c axis) is perpendicular to one of the rectangular faces of the prism side, and the other two prism edges, X and Y, are then oriented normal to the optic axis. According to the minimum deviation principle, the refractive index can be calculated by the equation[13]

$$n = \sin\frac{A+D}{2}/\sin\frac{A}{2} \quad (5)$$

where A is the vertex angle of the prism, which is 39° in this experiment, and D is the minimum deviation angle. The values of room-temperature refractive indices for both the ordinary and the extraordinary polarizations measured at specific wavelengths are shown in Table 4 and Figure 5, in which the refractive index is plotted versus wavelength. The solid curve in Figure 5 represents the Sellmeier fit to the data. The Sellmeier equations, which are fitted by the least-squares method with the above-measured refractive indices, are given as follows

$$n_e^2 = 2.61324 + \frac{0.0236202}{\lambda^2 + 0.02148964}$$

$$n_o^2 = 2.66665 + \frac{0.024713}{\lambda^2 + 0.02426332}$$

where λ is the wavelength expressed in micrometers. The values calculated from them are consistent with the experimental ones to the third decimal place. The NBAC crystal is negative uniaxial with a relatively small birefringence. The magnitude of the refractive-index anisotropy δn increases with decreasing wavelength. From the above equations, the refractive indices at other wavelengths can be calculated. For example, at 808 nm, n_e = 1.627 and n_o = 1.644. This result is necessary for further calculation of the spectrum parameters and phase-matching situations.

Table 4. Refractive Indices of the NBAC Crystal

wavelength (nm)	n_e	n_o	δn
404.7	1.65612	1.67330	0.0172
435.8	1.65071	1.66792	0.0172
486.1	1.64418	1.66131	0.0171
491.6	1.64383	1.66096	0.0171
546.1	1.63907	1.65611	0.0170
578.0	1.63686	1.65392	0.0171
589.3	1.63614	1.65315	0.0170
656.3	1.63277	1.64960	0.0168
690.7	1.63127	1.64821	0.0169
694.3	1.63131	1.64803	0.0167
807.2	1.62719	1.64400	0.0168
861.7	1.62617	1.64284	0.0167
959.2	1.62410	1.64086	0.0168
1014	1.62327	1.64001	0.0167
1068	1.62245	1.63915	0.0167

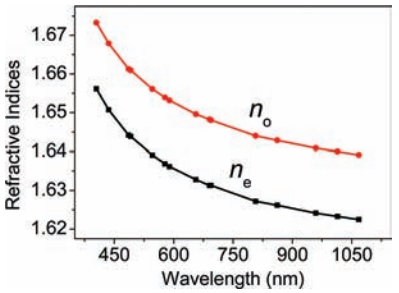

Figure 5. Refractive index dispersion curves of NBAC crystal. Points are experimental values; curves are the fits given by the Sellmeier equation.

Figure 6 shows the DSC curve of NBAC crystal grown from NaF−LiCl flux. From Figure 6, a single sharp endothermic peak was observed in the temperature range from 930.0 to 980.0 °C. This peak exhibits the characteristics of a first-order phase transition with a peak temperature at 971.6 °C. Evidence of the fusion of the NBAC crystal was found in the sample cell after DSC measurement. The transition can be ascribed to a solid-to-liquid phase change. The sharp peak temperature of 971.6 °C was identified as the melting point of the crystal. We also performed DSC experiments on the NBAC crystal grown from single LiCl flux and the polycrystalline NBAC fabricated by the solid state synthesis with stoichiometry composition. The results show that the melting point of NBAC grown from NaF−LiCl flux is 8 and 7.4 °C higher than that of polycrystalline NBAC and NBAC crystals grown from LiCl flux, respectively.

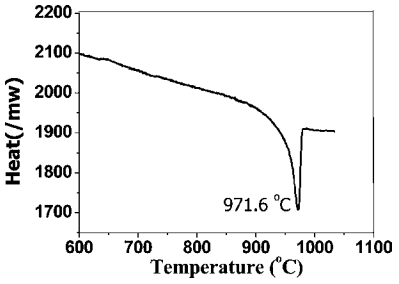

Figure 6. DSC curve for NBAC crystal grown from NaF−LiCl flux.

dx.doi.org/10.1021/ic300306v | Inorg. Chem. 2012, 51, 6682−6686

The difference indicated that the purity and quality of NBAC crystal grown from NaF−LiCl flux might be higher than that of polycrystalline NBAC and NBAC crystals grown from single LiCl flux.

Figure 7 shows the thermal-expansion versus temperature curves along *a* and *c* crystallographic directions. The crystal

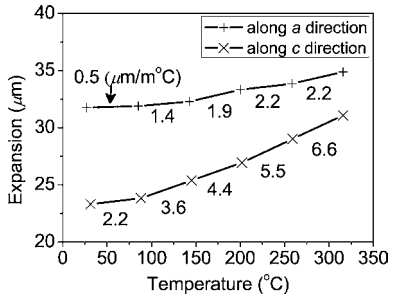

Figure 7. Thermal expansion curves of NBAC crystal.

exhibits only expansion when it is heated, which means that all the thermal-expansion coefficients are positive. The average linear thermal-expansion coefficients in the temperature range from 20 to 300 °C were calculated to be $\alpha_a = 1.6 \times 10^{-6}/°C$ and $\alpha_c = 4.5 \times 10^{-6}/$ °C along the *a* and *c* crystallographic directions, respectively. These results indicate that $\alpha_c/\alpha_a \approx 2.8$ and suggest that the crystal possesses a large anisotropic thermal expansion. During crystal growth, anisotropic thermal expansion will cause large thermal stress in the crystal, especially when the crystal grows larger or when the temperature varies. For NBAC, the maximum and minimum thermal expansion will occur in the direction of the *c* and *a* axes, respectively. The *c*-axis dimension will lengthen to approximately 2.8 times that along the *a* axis. Therefore, the crystal should be cooled to room temperature at a low rate after growth; otherwise, the crystal will more than likely crack. In our crystal growth experiment, the cooling rate is less than 40 °C/h and a large-size high-quality NBAC crystal was obtained as shown in Figure 1.

CONCLUSION

NBAC crystals with large sizes up to 34 × 34 × 16 mm^3 have been successfully grown by the top-seeded solution growth method using NaF−LiCl as the flux. The crystal structure has been studied. Its main structural element is a $[AlB_4O_{12}]^{9-}$, group which is formed by two BO_4 tetrahedra, one AlO_4 tetrahedra, as well as two BO_3 triangles with shared O atoms. NBAC crystal is transparent down to 230 nm. The refractive indices were measured, and the Sellmeier equations were fitted. The melting point was measured to be 971.6 °C. The average linear thermal-expansion coefficients were measured to be $\alpha_a = 1.6 \times 10^{-6}/°C$ and $\alpha_c = 4.5 \times 10^{-6}/$ °C, indicating that the NBAC crystal possesses a large anisotropic thermal expansion.

ASSOCIATED CONTENT

Supporting Information

Crystal data in CIF format including the refined atomic positions, isotropic thermal parameters, and main interatomic distances etc. This material is available free of charge via the Internet at http://pubs.acs.org.

AUTHOR INFORMATION

Corresponding Author

*E-mail: zjx@mail.ipc.ac.cn.

Notes

The authors declare no competing financial interest.

ACKNOWLEDGMENTS

This work was supported by the National Basic Research Project of China (No. 2010CB630701) and the National Natural Science Foundation of China (No. 50802100). Jianxiu Zhang thanks the Alexander von Humboldt Foundation for all support during her research in Germany.

REFERENCES

(1) Sasaki, T.; Mori, Y.; Yoshimura, M.; Yap, Y. K.; Kamimura, T. *Mater. Sci. Eng. Rep.* **2000**, *30* (1−2), 1.
(2) Dewey, C. F.; Cook, W. R.; Hodgson, R. T.; Wynne, J. J. *Appl. Phys. Lett.* **1975**, *26* (12), 714.
(3) Chen, C. T.; Wu, B. C.; Jiang, A. D.; You, G. M. *Sci. Sin. [B]* **1985**, *28*, 235.
(4) Chen, C. T.; Wu, Y. C.; Jiang, A. D.; Wu, B. C.; You, G. M.; Li, R. K.; Lin, S. J. *J. Opt. Soc. Am. B* **1989**, *6* (4), 616.
(5) Wu, Y. C.; Sasaki, T.; Nakai, S.; Yokotani, A.; Tang, H. G.; Chen, C. T. *Appl. Phys. Lett.* **1993**, *62* (21), 2614.
(6) Iwai, M.; Kobayashi, M.; Furuya, H.; Mori, Y.; Sasaki, T. *Jpn. J. Appl. Phys.* **1997**, *36*, L276.
(7) Zhang, S. F.; Wu, Y. C.; Li, Y. G.; Fu, P. Z. *J. Syn. Cryst. (in Chinese)* **2007**, *36* (4), 719.
(8) Goryynova, N. A.; Borshchevskii, A. S.; Tretiakov, P. N. *Semiconductor and Semimetal*; Academic Press: New York, 1968.
(9) Winkler, H. G. F. *Structure and Characteristic of Crystal*; Science Press: Beijing, 1960.
(10) Touboul, M.; Penin, N.; Nowogrocki, G. *J. Solid State Chem.* **2000**, *342*, 150.
(11) Chenavas, J.; Grey, I.; Guitel, J.; Joubert, J.; Marezio, M. *Acta Crystalllogr.* **1981**, *1343*, B37.
(12) Hu, Z. G.; Maramatsu, K.; Kanehisa, N.; Yoshimmura, M.; Mori, Y.; Sasaki, T.; Kai, Y. *Z. Kristallogr.-New Cryst. Struct.* **2003**, *218*, 1.
(13) Lotem, H.; Burshtein, Z. *Opt. Lett.* **1987**, *12*, 561.